

Magnetoresistance in the SDW state of $(\text{TMTSF})_2\text{PF}_6$ above $T^* \approx 4\text{ K}$; Novel effect due to the Landau quantization

B. KORIN-HAMZIĆ^{1(*)}, M. BASLETIĆ² and K. MAKI³

¹ *Institute of Physics, POB 304, HR-10001 Zagreb, Croatia*

² *Department of Physics, Faculty of Science, POB 331, HR-10001 Zagreb, Croatia*

³ *Department of Physics, University of Southern California, Los Angeles CA 90089-0484, USA and Max-Planck Institute for the Physics of Complex Systems, Nöthnitzer Str.38, D-01187 Dresden, Germany*

PACS. 75.30.F – Spin density wave.

PACS. 72.15.Gd – Galvanomagnetic and other magnetotransport effects.

PACS. 72.80.Le – Polymers and Organic conductors.

Abstract. – Magnetoresistance in the spin-density wave (SDW) state of $(\text{TMTSF})_2\text{PF}_6$ is known to exhibit a rich variety of the angular dependencies when a magnetic field \mathbf{B} is rotated in the $\mathbf{b}'\text{-c}^*$, $\mathbf{a}\text{-b}'$ and $\mathbf{a}\text{-c}^*$ planes. In the presence of a magnetic field the quasiparticle spectrum in the SDW with imperfect nesting is quantized. In such a case the minimum quasiparticle energy depends both on the magnetic field strength $|B|$ and the angle θ between the field and the crystal direction \mathbf{a} , \mathbf{b}' or \mathbf{c}^* . This approach describes rather satisfactory the magnetoresistance above $T^* \approx 4\text{ K}$.

Introduction. – Since the discovery of the superconductivity in $(\text{TMTSF})_2\text{PF}_6$ in 1979 [1] the Bechgaard salts or the highly anisotropic organic conductors $(\text{TMTSF})_2\text{X}$ (where TMTSF is tetramethyltetraselenafulvalene and X is anion PF_6 , AsF_6 , $\text{ClO}_4 \dots$) are well known because of a variety of physical phenomena related to their low dimensionality. Their rich phase diagram exhibits various low temperature phases under pressure and/or in magnetic field among which the spin density wave (SDW), field induced SDW (FISDW) with quantum Hall effect, and unconventional superconductivity are the most intriguing [2,3]. The quasi-one-dimensionality (1D) is a consequence of the crystal structure, where the TMTSF molecules are stacked in columns in the \mathbf{a} direction (along which the highest conductivity occurs), and the resulting anisotropy in conductivity is commonly taken to be $\sigma_a : \sigma_b : \sigma_c \approx t_a^2 : t_b^2 : t_c^2 \approx 10^5 : 10^3 : 1$, where t_i are the tight binding transfer integrals. These materials are open-orbit metals with the Fermi surface (FS) consisting of a pair of weakly modulated sheets in the \mathbf{b} and \mathbf{c} directions.

The SDW ground state of the organic conductors $(\text{TMTSF})_2\text{X}$ has been the subject of considerable experimental and theoretical investigations in the last twenty years [2]. It is

(*) E-mail: bhamzic@ifs.hr

caused by the almost perfect nesting of the two sheets of the FS, due to the instability of the (1D) electron gas with strong electron-electron interactions. The opening of the energy gap (Δ) in the conduction band leads to the semiconducting transport properties. The external pressure increases the transverse coupling and above about 8 kbars the SDW ground state is suppressed in favor of superconductivity.

One of the most intriguing features of the $(\text{TMTSF})_2\text{X}$ is their anomalous behaviour in a magnetic field. There are several angular effects of magnetoresistance known in the literature, like the variety of resonance-like features, known as the geometrical resonance or the Lebed resonance (or the magic angle effect) [4], the Danner-Chaikin oscillation [5] and the third angular effect [6], and all of them are mostly connected with the metallic phase of $(\text{TMTSF})_2\text{X}$. Only few measurements of the magnetoresistance anisotropy, as far as we know, have been performed in the SDW ground state at ambient pressure [7–10].

$(\text{TMTSF})_2\text{PF}_6$ is one of the most investigated $(\text{TMTSF})_2\text{X}$ compound. It is metallic down to $T_{\text{SDW}} \approx 12\text{ K}$ where the metal-semiconductor transition into SDW ground state occurs and below which the resistance displays an activated behavior. It is known that SDW in $(\text{TMTSF})_2\text{PF}_6$ undergoes another transition at $T^* \approx T_{\text{SDW}}/3$ (at 3.5 – 4 K at ambient pressure) [4, 5], but the nature of the possible subphases remains controversial. We have recently shown [9–11] that the temperature dependent magnetoresistance anisotropy changes abruptly below 4 K, indicating a possible phase transition at $T^* \approx 4\text{ K}$.

In this paper we shall concentrate ourselves to the magnetoresistance (MR) behavior above T^* , and we propose that it can be understood in terms of the Landau quantization of the quasiparticle spectrum in a magnetic field B , where the imperfect nesting plays the crucial role. The experimental MR data of $(\text{TMTSF})_2\text{PF}_6$ at $T = 4.2\text{ K}$ will be compared with our new theoretical model. The discussion of the magnetoresistance below T^* , in terms of unconventional SDW (or USDW), will be presented elsewhere [11, 12].

Experiment. – The measurements were done in magnetic fields up to 5 T with directions of the current along the different crystal axis, and for different orientations of the applied magnetic field. A rotating sample holder enabled the sample rotation around a chosen axis over a range of 190° . The experimental MR data are for \mathbf{c}^* ($\mathbf{j} \parallel \mathbf{c}^*$), \mathbf{b}' ($\mathbf{j} \parallel \mathbf{b}'$) and \mathbf{a} ($\mathbf{j} \parallel \mathbf{a}$) axis and for different orientations of magnetic field. The single crystals used come all from the same batch. Their \mathbf{a} direction is the highest conductivity direction, the \mathbf{b}' direction (with intermediate conductivity) is perpendicular to \mathbf{a} in the $\mathbf{a}\text{-}\mathbf{b}'$ plane, and \mathbf{c}^* direction (with the lowest conductivity) is perpendicular to the $\mathbf{a}\text{-}\mathbf{b}'$ plane (and $\mathbf{a}\text{-}\mathbf{b}$). The room temperature conductivity values are: $\sigma_a = 500 (\Omega\text{ cm})^{-1}$, $\sigma_b = 20 (\Omega\text{ cm})^{-1}$ and $\sigma_c = 1/35 (\Omega\text{ cm})^{-1}$.

The MR (defined as $\Delta\rho/\rho_0 = [\rho(B) - \rho(0)]/\rho(0)$) was measured in various four probe

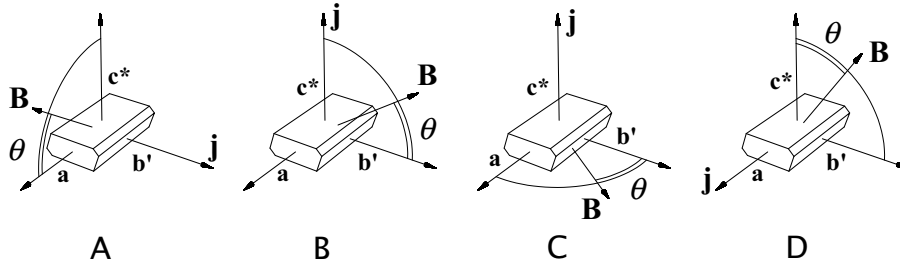


Fig. 1 – Four configurations (A, B, C and D) of the current \mathbf{j} and magnetic field \mathbf{B} direction. (See text for a detailed explanation.)

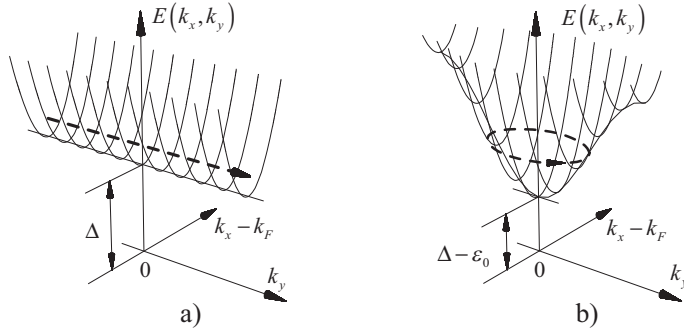


Fig. 2 – $E(k_x, k_y)$ in SDW with a) perfect nesting, and b) imperfect nesting.

arrangements on samples cut from the long crystals. In the case of ρ_a ($\mathbf{j} \parallel \mathbf{a}$), ρ_b ($\mathbf{j} \parallel \mathbf{b}'$) and ρ_c ($\mathbf{j} \parallel \mathbf{c}^*$), two pairs of the contacts were placed on the opposite $\mathbf{b}'\text{-}\mathbf{c}^*$, $\mathbf{a}\text{-}\mathbf{c}^*$ and $\mathbf{a}\text{-}\mathbf{b}'$ surfaces, respectively.

The four configurations that will be analyzed in this work are shown on Fig 1A, B, C and D:

i) Fig. 1A shows the case when the current direction is along the \mathbf{b}' axis and the magnetic field is rotated in the $\mathbf{a}\text{-}\mathbf{c}^*$ plane ($\mathbf{j} \parallel \mathbf{b}'$, $\mathbf{B} \parallel (\mathbf{a}\text{-}\mathbf{c}^*)$) perpendicular to the current direction. θ is the angle between \mathbf{B} and the \mathbf{a} axis, *i.e.* $\theta = 0$ for $\mathbf{B} \parallel \mathbf{a}$ and $\theta = 90^\circ$ for $\mathbf{B} \parallel \mathbf{c}^*$.

ii) Fig. 1B shows the case when the current direction is along the \mathbf{c}^* axis and the magnetic field is rotated in the $\mathbf{b}'\text{-}\mathbf{c}^*$ plane ($\mathbf{j} \parallel \mathbf{c}^*$, $\mathbf{B} \parallel (\mathbf{b}'\text{-}\mathbf{c}^*)$). θ is the angle between \mathbf{B} and the \mathbf{b}' axis, *i.e.* $\theta = 0$ for $\mathbf{B} \parallel \mathbf{b}'$ and $\theta = 90^\circ$ for $\mathbf{B} \parallel \mathbf{c}^*$.

iii) Fig. 1C shows the case when the current direction is along the \mathbf{c}^* axis and the magnetic field is rotated in the $\mathbf{a}\text{-}\mathbf{b}'$ plane ($\mathbf{j} \parallel \mathbf{c}^*$, $\mathbf{B} \parallel (\mathbf{a}\text{-}\mathbf{b}')$) perpendicular to the current direction. θ is the angle between \mathbf{B} and the \mathbf{b}' axis, *i.e.* $\theta = 0$ for $\mathbf{B} \parallel \mathbf{b}'$ and $\theta = 90^\circ$ for $\mathbf{B} \parallel \mathbf{a}$.

iv) Fig. 1D shows the case when the current direction is along the \mathbf{a} axis and the magnetic field is rotated in the $\mathbf{b}'\text{-}\mathbf{c}^*$ plane ($\mathbf{j} \parallel \mathbf{a}$, $\mathbf{B} \parallel (\mathbf{b}'\text{-}\mathbf{c}^*)$) perpendicular to the current direction. θ is the angle between \mathbf{B} and the \mathbf{c}^* axis, *i.e.* $\theta = 0$ for $\mathbf{B} \parallel \mathbf{c}^*$ and $\theta = 90^\circ$ for $\mathbf{B} \parallel \mathbf{b}'$.

Model, Results and Discussion. – If we limit ourselves to SDW above $T^* \approx 4$ K, it is well established that the quasiparticle energy is given by [9, 13]:

$$E(\mathbf{k}) = \sqrt{\eta^2 + \Delta^2} - \varepsilon_0 \cos 2bk_y, \quad (1)$$

where $\eta = \sqrt{v_a^2 (k_x - k_F)^2 + v_c^2 k_z^2}$ is the quasiparticle energy in the normal state (v_a and v_c are Fermi velocities in \mathbf{a} and \mathbf{c}^* direction), $\Delta \approx 34$ K is the order parameter for SDW and $\varepsilon_0 \approx 13$ K is the parameter characterizing the imperfect nesting [9]. In a presence of a magnetic field B the quasiparticle orbit is quantized. This can be readily seen from the quasiparticle energy landscape as shown in Fig. 2. In Fig. 2a we show the quasiparticle energy for SDW with perfect nesting. Quasiparticle energy has the minima at $k_x = \pm k_F$, which is independent of k_y and consequently, the quasiparticle orbit is open. On the other hand, for SDW with imperfect nesting, there are minima for quasiparticle energy at $k_x = \pm k_F$ and $k_y = \pm \pi/2b$ (see Fig. 2b). Therefore, in the presence of a magnetic field, quasiparticle will circle around these minima, *i.e.* closed orbits appear and they will be quantized.

We expand the quasiparticle energy in Eq. (1) for small $(k_x - k_F)^2$ and k_y^2 . In the presence of a magnetic field within different planes (Fig. 1) the minimum quasiparticle energy (*i.e.* the

energy gap) associated with the lowest Landau level is given by:

$$E(B, \theta) = \Delta - \varepsilon_0 + \sqrt{\frac{\varepsilon_0}{\Delta}} v_a b e B \sqrt{\sin^2 \theta + \gamma_2 \cos^2 \theta}, \quad \text{for } \mathbf{B} \parallel (\mathbf{b}' - \mathbf{c}^*) \quad (2)$$

$$= \Delta - \varepsilon_0 + \frac{v_a v_c b e}{2\Delta} B \sqrt{\sin^2 \theta + \gamma_3 \cos^2 \theta}, \quad \text{for } \mathbf{B} \parallel (\mathbf{a} - \mathbf{b}') \quad (3)$$

$$= \Delta - \varepsilon_0 + \sqrt{\frac{\varepsilon_0}{\Delta}} v_a b e B |\sin \theta|, \quad \text{for } \mathbf{B} \parallel (\mathbf{a} - \mathbf{c}^*), \quad (4)$$

where $\gamma_2 = \gamma_3^{-1} = (v_c/2b)^2 / \varepsilon_0 \Delta$. In general, the quasiparticle energy gap increases linearly with $|B|$ and depends on angle θ (as defined in Fig. 1). For $B = 0$ the resistance is given as $\rho_i \propto \exp[\beta E(0, 0)]$. For $B \neq 0$ and for $\omega_c \tau > 1$ (ω_c - cyclotron frequency; τ - scattering rate; we also assume that the quasiparticle scattering rate is independent of \mathbf{k}) we may write down the magnetoresistance as:

$$\rho_{zz}(T, B) = \exp \left\{ \beta(\Delta - \varepsilon_0) \left[1 + A_2 B \sqrt{\sin^2 \theta + \gamma_2 \cos^2 \theta} \right] \right\} \\ \times \left(1 + C_2 B \sqrt{\sin^2 \theta + \gamma_2 \cos^2 \theta} \right), \quad \text{for } \mathbf{B} \parallel (\mathbf{b}' - \mathbf{c}^*) \quad (5)$$

$$\rho_{zz}(T, B) = \exp \left\{ \beta(\Delta - \varepsilon_0) \left[1 + A_3 B \sqrt{\sin^2 \theta + \gamma_3 \cos^2 \theta} \right] \right\} \\ \times \left(1 + C_3 B \sqrt{\sin^2 \theta + \gamma_3 \cos^2 \theta} \right), \quad \text{for } \mathbf{B} \parallel (\mathbf{a} - \mathbf{b}'), \quad (6)$$

with:

$$A_2 = \sqrt{\frac{\varepsilon_0}{\Delta}} \frac{v_a b e}{\Delta - \varepsilon_0}, \quad A_3 = \frac{v_a v_c e}{2\Delta} \frac{1}{\Delta - \varepsilon_0}. \quad (7)$$

We compare now our experimental data with the above equations. Figs. 3 and 4 show magnetic field dependence of MR ($\mathbf{j} \parallel \mathbf{c}^*$, $\mathbf{B} \parallel \mathbf{c}^*$ and $\mathbf{B} \parallel \mathbf{b}'$) and the angular dependence of MR ($\mathbf{j} \parallel \mathbf{c}^*$, $\mathbf{B} \parallel (\mathbf{b}' - \mathbf{c}^*)$) at 4.2 K, respectively. The solid lines are fits to Eq. (5). The analogous results for $\mathbf{j} \parallel \mathbf{c}^*$ but different magnetic field rotation ($\mathbf{B} \parallel (\mathbf{a} - \mathbf{b}')$) is given on Figs. 5 and 6. The solid lines are fits to Eq. (6).

On the other hand, for $\mathbf{j} \parallel \mathbf{b}'$ and $\mathbf{B} \parallel (\mathbf{a} - \mathbf{c}^*)$ we obtain:

$$\frac{\Delta \rho_{yy}(T, B)}{\rho_{yy}(T, 0)} = \exp \{ \beta(\Delta - \varepsilon_0) A_1 B |\sin \theta| \} (1 + C_1 B |\sin \theta|), \quad (8)$$

where $A_1 = \sqrt{\varepsilon_0/\Delta} v_a b e / (\Delta - \varepsilon_0)$. We give the excess magnetoresistance rather than the MR itself, as in this configuration the quasiparticle energy gap for $B = 0$ is only 8 K [9], instead of all other cases where $\Delta - \varepsilon_0 = 21$ K. The experimental results for $\mathbf{j} \parallel \mathbf{b}'$ and \mathbf{B} in $\mathbf{a} - \mathbf{c}^*$ plane are shown on Figs. 7 and 8. The solid lines are fits to Eq. (8).

It is evident that the present model (Eq. (5–8)) describes both the B and θ dependence of MR rather well (fits on Figs. 3–8 are from good to excellent). The fitting procedure yielded $\Delta - \varepsilon_0 = 21$ K, $A_2 = 0.014 \text{ T}^{-1}$, $\gamma_2 = 0.85$, $C_2 = 0.38 \text{ T}^{-1}$, $A_3 = 0.00905 \text{ T}^{-1}$, $\gamma_3 = 3.1$, $C_3 = 0$, $A_1 = 0.048 \text{ T}^{-1}$, $C_1 = 2.14 \text{ T}^{-1}$.

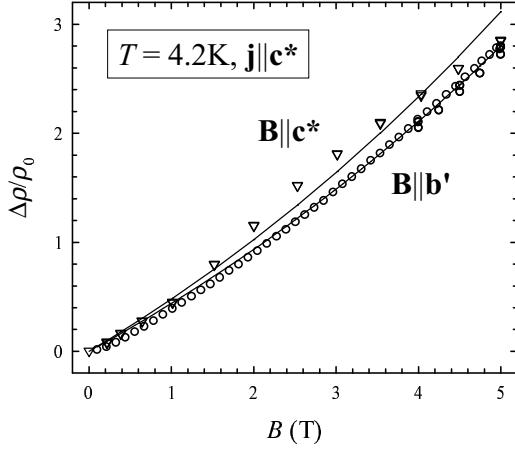


Fig. 3

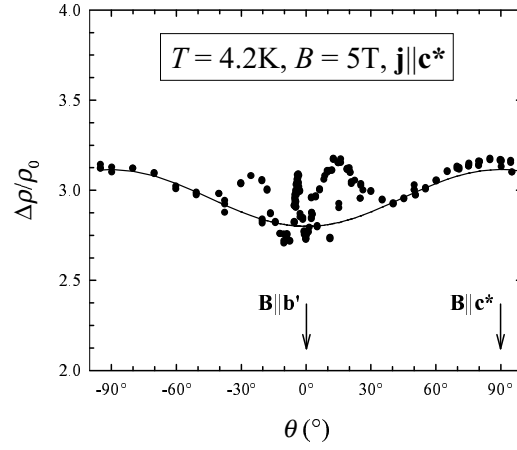


Fig. 4

Fig. 3 – Magnetic field dependence of $\Delta\rho/\rho_0$ at 4.2 K for $\mathbf{j}\parallel\mathbf{c}^*$, $\mathbf{B}\parallel\mathbf{b}'$ and $\mathbf{B}\parallel\mathbf{c}^*$ (see Fig. 1B). Solid lines are fits to the theory (see text).

Fig. 4 – Angular dependence of $\Delta\rho/\rho_0$ at 4.2 K and $B = 5$ T, for $\mathbf{j}\parallel\mathbf{c}^*$, \mathbf{B} in $\mathbf{b}'\text{-}\mathbf{c}^*$ plane (see Fig. 1B). Solid lines are fits to the theory (see text).

First, from A_2 and γ_2 we can extract the \mathbf{a} axis coherence length $\xi_a = v_a/\Delta = 120$ Å and $v_c/v_a = 7.33 \times 10^{-2}$. The ratio v_c/v_a appears to be somewhat larger than the one previously determined ($v_c/v_a = 1.7 \times 10^{-2}$ [2]) but the difference is minor. Furthermore, A_3 gives $\xi_a = 100$ Å, where we used our v_c/v_a value. We can, therefore, conclude that ξ_a is

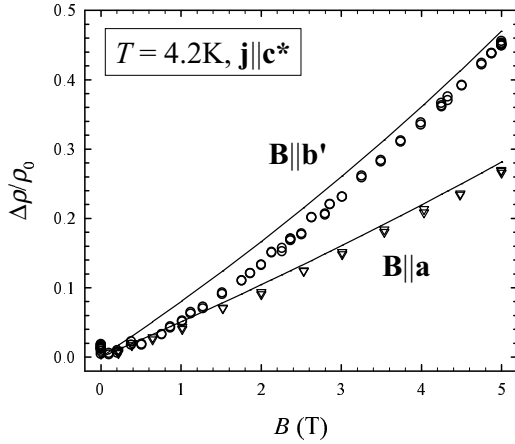


Fig. 5

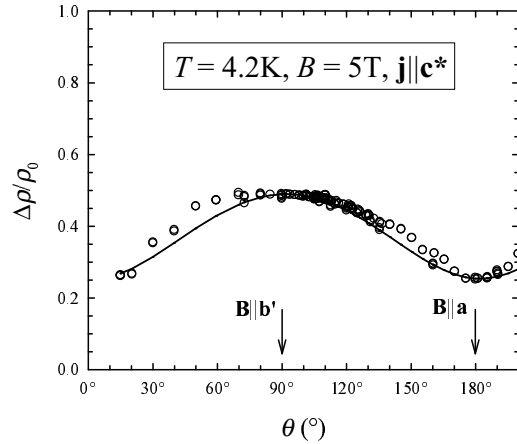


Fig. 6

Fig. 5 – Magnetic field dependence of $\Delta\rho/\rho_0$ at 4.2 K for $\mathbf{j}\parallel\mathbf{c}^*$, $\mathbf{B}\parallel\mathbf{a}$ and $\mathbf{B}\parallel\mathbf{b}'$ (see Fig. 1C). Solid lines are fits to the theory (see text).

Fig. 6 – Angular dependence of $\Delta\rho/\rho_0$ at 4.2 K and $B = 5$ T, for $\mathbf{j}\parallel\mathbf{c}^*$, \mathbf{B} in $\mathbf{a}\text{-}\mathbf{b}'$ plane (see Fig. 1C). Solid lines are fits to the theory (see text).

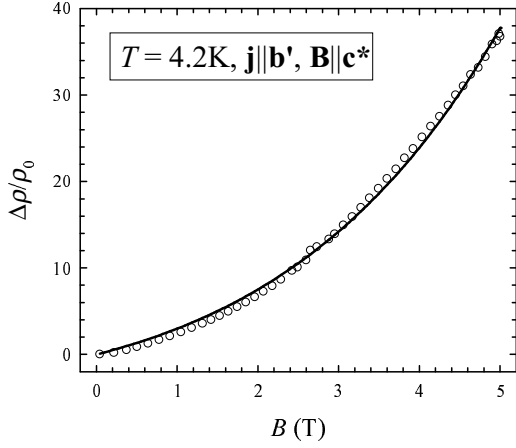


Fig. 7

Fig. 7 – Magnetic field dependence of $\Delta\rho/\rho_0$ at 4.2 K for $\mathbf{j}\parallel\mathbf{b}'$, $\mathbf{B}\parallel\mathbf{c}^*$ (see Fig. 1A). Solid lines are fits to the theory (see text).

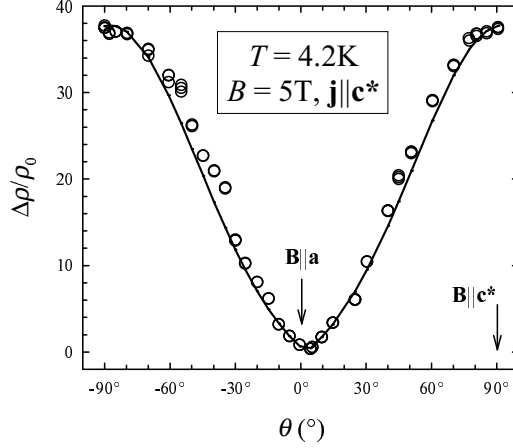


Fig. 8

Fig. 8 – Angular dependence of $\Delta\rho/\rho_0$ at 4.2 K and $B = 5$ T, for $\mathbf{j}\parallel\mathbf{b}'$, \mathbf{B} in $\mathbf{a}-\mathbf{c}^*$ plane (see Fig. 1A). Solid lines are fits to the theory (see text).

consistent in these two configurations. On the other hand, γ_3 gives $\xi_a = 5.4 \text{ \AA}$ (the value that appears to be too small) and A_1 gives $\xi_a = 410 \text{ \AA}$ (which is somewhat larger, but the difference of a factor 3.5 may be acceptable).

Finally, we comment the result for the highest conductivity direction \mathbf{a} , *i.e.* $\rho_{xx}(T, B)$

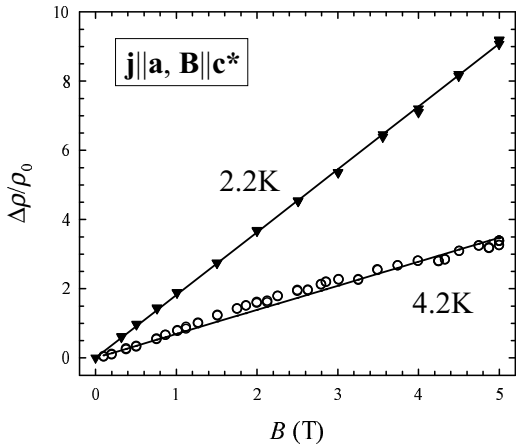


Fig. 9

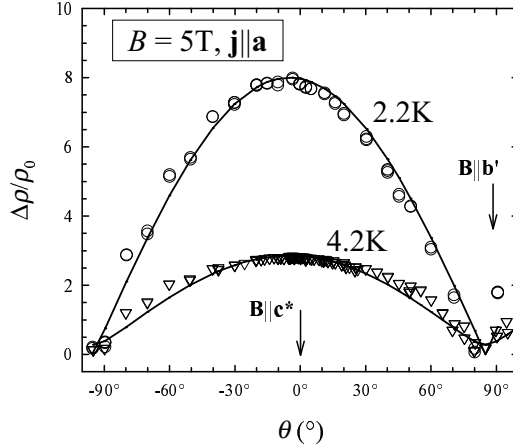


Fig. 10

Fig. 9 – Magnetic field dependence of $\Delta\rho/\rho_0$ at 4.2 K and 2.2 K, for $\mathbf{j}\parallel\mathbf{a}$, $\mathbf{B}\parallel\mathbf{c}^*$ (see Fig. 1D). Solid lines are fits to the theory (see text).

Fig. 10 – Angular dependence of $\Delta\rho/\rho_0$ at 4.2 K and 2.2 K, for $B = 5$ T and $\mathbf{j}\parallel\mathbf{a}$, \mathbf{B} in $\mathbf{b}'-\mathbf{c}^*$ plane (see Fig. 1D). Solid lines are fits to the theory (see text).

for \mathbf{B} in the $\mathbf{b}'\text{-}\mathbf{c}^*$ plane, perpendicular to the current direction. The experimental results for the magnetic field dependence of MR ($\mathbf{j}\parallel\mathbf{a}$, $\mathbf{B}\parallel\mathbf{c}^*$ at 4.2 K and 2.2 K) and the angular dependence of MR at 4.2 K and 2.2 K are shown on Figs. 9 and 10. We notice that the angular dependencies of MR for $T = 4.2$ K and 2.2 K look very similar (see Fig. 10). Namely, the fitted $\rho_{xx}(T, B)$ for both $T = 4.2$ K and 2.2 K (Figs. 9 and 10, solid lines), are well accounted for by:

$$\rho_{xx}(B, \theta) \propto 1 + C_1 B |\cos \theta|, \quad (9)$$

where θ is the angle $\angle(\mathbf{B}, \mathbf{c}^*)$. Here $C_1 = 0.55 \text{ T}^{-1}$ and 1.6 T^{-1} for $T = 4.2$ K and 2.2 K, respectively.

The linear B dependence of ρ_{xx} for $\mathbf{B}\parallel(\mathbf{b}'\text{-}\mathbf{c}^*)$ in SDW state of $(\text{TMTSF})_2\text{PF}_6$ (Fig. 9) is well known [2], though it is not understood. Therefore, we may conclude that $\rho_{xx}(T, B)$ is not sensitive to the quasiparticle spectrum we are considering here.

Conclusion. – In summary, we have derived the expression of the magnetoresistance based on the Landau quantization of the quasiparticle orbit in SDW with imperfect nesting. At the qualitative level these expressions give excellent description of experimental magnetoresistance results. From fitting procedure, we can deduce the physical content like ξ_a and v_c/v_a , which both look very reasonable. The origin of a few cases where ξ_a has not a consistent value remains to be clarified. In any case, we may conclude that the Landau quantization of the quasiparticle energy describes most of salient features of the angular dependence of the magnetoresistance in SDW in $(\text{TMTSF})_2\text{PF}_6$ above $T^* \approx 4$ K.

A parallel study of the magnetoresistance for $T < T^*$ based on possible USDW in addition to the already existing SDW, will be reported elsewhere [11, 12].

* * *

This experimental work was performed on samples prepared by K. Bechgaard. We acknowledge useful discussion with A. Hamzić and S. Tomić.

REFERENCES

- [1] JÉROME D., MAZAUD A., RIBAUT M. and BECHGAARD K., *J. Phys. (Lettres)*, **41** (1980) L-95
- [2] ISHIGURO T., YAMAJI K. and SAITO G., *Organic superconductors*, (Springer) 1998, 2nd ed.
- [3] LEE I. J., BROWN S. E., CLARK W. K., STROUSE J., NAUGHTON M. J., KANG W. and CHAIKIN P. M., *Phys. Rev. Lett.*, **88** (2002) 017004
- [4] LEBED A. G., *JETP Lett.*, **43** (1986) 174; CHAIKIN P. M., *J. Phys. I (France)*, **6** (1996) 1875
- [5] DANNER G. M. and CHAIKIN P. M., *Phys. Rev. Lett.*, **75** (1995) 4690
- [6] OSADA T., KAGOSHIMA S. and MIURA N., *Phys. Rev. Lett.*, **77** (1996) 5261
- [7] ULMET J. P., AUBAN P., KHMOU A. and ASKENAZY S., *J. Phys. Lett.*, **46** (1985) L535
- [8] BASLETIĆ M., BIŠKUP N., KORIN-HAMZIĆ B., TOMIĆ S., HAMZIĆ A., BECHGAARD K. and FABRE J. M., *Europhys. Lett.*, **22** (1993) 279
- [9] KORIN-HAMZIĆ B., BASLETIĆ M. and MAKI K., *Europhys. Lett.*, **43** (1998) 450
- [10] KORIN-HAMZIĆ B., BASLETIĆ M., FRANCETIĆ N., HAMZIĆ A., and BECHGAARD K., *J. Phys. IV France*, **9** (1999) Pr10;247
- [11] BASLETIĆ M., KORIN-HAMZIĆ B. and MAKI K., submitted to *Phys. Rev. B*
- [12] KORIN-HAMZIĆ B., BASLETIĆ M. and MAKI K., submitted to *Int. J. Mod. Phys. B*
- [13] HUANG X. and MAKI K., *Phys. Rev. B*, **42** (1990) 6498